PHYSICS

Self-testing nonprojective quantum measurements in prepare-and-measure experiments

Armin Tavakoli[1]*, **Massimiliano Smania**[2], **Tamás Vértesi**[3], **Nicolas Brunner**[1], **Mohamed Bourennane**[2]

Self-testing represents the strongest form of certification of a quantum system. Here, we theoretically and experimentally investigate self-testing of nonprojective quantum measurements. That is, how can one certify, from observed data only, that an uncharacterized measurement device implements a desired nonprojective positive-operator valued measure (POVM). We consider a prepare-and-measure scenario with a bound on the Hilbert space dimension and develop methods for (i) robustly self-testing extremal qubit POVMs and (ii) certifying that an uncharacterized qubit measurement is nonprojective. Our methods are robust to noise and thus applicable in practice, as we demonstrate in a photonic experiment. Specifically, we show that our experimental data imply that the implemented measurements are very close to certain ideal three- and four-outcome qubit POVMs and hence non-projective. In the latter case, the data certify a genuine four-outcome qubit POVM. Our results open interesting perspective for semi–device-independent certification of quantum devices.

INTRODUCTION

Measurements in quantum theory were initially represented by complete sets of orthogonal projectors on a Hilbert space. Such measurements are standard in a multitude of applications. Nevertheless, in a modern understanding of quantum theory, measurements are described by positive-operator valued measures (POVMs), i.e., a set of positive semi-definite operators summing to identity. POVMs are the most general notion of a quantum measurement; all projective measurements are POVMs, but not all POVMs need be projective.

Nonprojective measurements are widely useful in both conceptual and applied aspects of quantum theory, as well as in quantum information processing. In several practically motivated tasks, they present concrete advantages over projective measurements. Nonprojective measurements enhance estimation and tomography of quantum states (*1*, *2*), as well as entanglement detection (*3*) and unambiguous state discrimination of nonorthogonal states (*4*, *5*). They have also found applications in quantum cryptography (*6*, *7*) and randomness generation (*8*). In addition, nonprojective measurements can be used to maximally violate particular Bell inequalities (*9*) (assuming a bound on the Hilbert space dimension), a fact that has been applied to improve randomness extraction beyond what is achievable with projective measurements (*10*, *11*).

In view of their diverse and growing applicability, it is important to develop tools for certifying and characterizing nonprojective measurements under minimal assumptions. The strongest possible form of certification involves a "black-box" scenario, where the quantum devices are a priori uncharacterized. Astonishingly, it is possible in certain cases to completely characterize both the quantum state and the measurements based only on observed data, which is referred to as "self-testing" (*12*). A well-known example is that the maximal violation of the Clauser-Horne-Shimony-Holt Bell inequality (*13*) implies (self-tests) a maximally entangled two-qubit state and pairs

of anticommuting local projective measurements (*14*–*16*). Self-testing can also be made robust to noise (*17*, *18*).

However, for the purpose of characterizing nonprojective measurements in the black-box scenario, methods based on Bell inequalities encounter a challenge. Because of Neumark's theorem, every nonprojective measurement can be recast as a projective measurement in a larger Hilbert space. That is, any nonprojective measurement on a given system is equivalent to projective measurement applied to the joint state of the system and an ancilla of a suitable dimension [see, e.g., (*19*)]. Since one usually considers no restriction on Hilbert space dimension in the Bell scenario, it is nontrivial to characterize a nonprojective measurement based on a Bell inequality. While this is possible in theory (in the absence of noise) (*10*), it appears challenging in the more realistic scenario where the experiment features imperfections. To the best of our knowledge, robust self-testing methods for nonprojective measurements in Bell scenarios have not yet been developed. A possible way to circumvent the problem is to consider a Bell scenario with quantum systems of bounded Hilbert space dimension. In particular, Gómez *et al.* (*11*) and Gómez *et al.* (*20*) recently reported the experimental certification of a nonprojective measurement in a Bell experiment assuming qubits. However, these experiments do not represent self-tests, as they certify the nonprojective character of a measurement, but not how it relates to a specific target POVM.

Here, we investigate the problem of self-testing nonprojective measurements under the assumption of bounded Hilbert space dimension. We follow a different approach, by considering a prepare-and-measure scenario instead of a Bell scenario. First, this scenario offers a natural framework for certifying and characterizing nonprojective measurements. The reason is that, as argued above, the notion of nonprojectiveness almost inherently involves a notion of Hilbert spaces of fixed dimension. Then, the prepare-and-measure scenario is arguably the simplest scenario in which the problem can be studied without further assumptions. Second, the prepare-and-measure scenario offers a very significant practical advantage as compared to Bell experiments. The reason is that there is no need to involve distant observers and entangled states. This makes prepare-and-measure scenarios simpler to implement (*21*–*26*). Moreover, prepare-and-measure scenarios are easier to analyze theoretically, which allows

[1]Département de Physique Appliquée, Université de Genève, CH-1211 Genève, Switzerland. [2]Department of Physics, Stockholm University, S-10691 Stockholm, Sweden. [3]MTA Atomki Lendület Quantum Correlations Research Group, Institute for Nuclear Research, Hungarian Academy of Sciences, H-4001 Debrecen, P.O. Box 51, Hungary.
*Corresponding author. Email: armin.tavakoli@unige.ch

us to develop self-testing methods that are versatile and highly robust to noise. Third, the assumption of a dimension bound is reasonable for characterization schemes. This is due to the fact that characterization schemes are not adversarial; i.e., they do not involve malicious devices. The experimenter typically knows which degrees of freedom are relevant; for example, the polarization of photons. However, every experiment is subject to unavoidable errors due, e.g., to technical noise and alignment errors. Characterization of quantum devices in this realistic setting is well captured by our assumption of a dimension bound.

In the first part of the paper, we present methods for characterizing nonprojective measurements. First, we present a method for self-testing a targeted nonprojective measurement in noiseless scenarios. Second, since noiseless statistics never occur in practice, we present methods for inferring a lower bound on the closeness of the uncharacterized measurement and a given target POVM, based on the observed noisy statistics; specifically, we lower-bound the worst-case fidelity between the real measurement and the ideal target one. Third, we introduce a method for determining whether the observed statistics could have arisen from some (unknown) projective measurements. If not, the measurement is certified as nonprojective. These methods have twofold relevance. On the one hand, they enable foundational insights into physical inference of nonprojective measurements in a semi–device-independent setting. On the other hand, they provide tools for assessing and certifying the quality of an experimental setup. We demonstrate the practicality of these self-testing methods in two experiments. In the first, we target a symmetric informationally complete (SIC) qubit POVM and demonstrate an estimated 98% worst-case fidelity. In addition, our data certify a genuine four-outcome qubit POVM. In the second experiment, we target a symmetric three-outcome qubit POVM and certify a worst-case fidelity of at least 96%. Last, we discuss some open questions.

THE SELF-TESTING PROBLEM, THE SCENARIO, AND OVERVIEW OF RESULTS

Self-testing is the task of characterizing a quantum system based only on observed data. In other words, it is about gaining knowledge of the physical properties of initially unknown states and/or measurements present in an experiment by studying the correlations observed in the laboratory.

In this work, we focus on prepare-and-measure scenarios. They differentiate themselves from Bell scenarios in two important ways. First, prepare-and-measure scenarios involve communicating observers and thus no space-like separation. Second, they do not involve entanglement, whereas Bell scenarios do. Prepare-and-measure scenarios can generally be modeled by two separated parties, Alice and Bob, who receive random inputs x and y, respectively. Alice prepares and sends a quantum state ρ_x to Bob who performs a measurement y with outcome b, represented by a POVM $\{M_y^b\}_b$ with

$$M_y^b \geq 0 \text{ and } \sum_b M_y^b = \mathbb{1} \ \forall y \tag{1}$$

This generates a probability distribution

$$P(b \mid x, y) = \text{tr}(\rho_x M_y^b) \tag{2}$$

To make the problem nontrivial, an assumption on Alice's preparations is required; otherwise, Alice could simply send x to Bob and

any probability distribution $P(b \mid x, y)$ would be achievable. The assumption we consider in this work is that Alice's preparations, i.e., the set of states ρ_x, can be represented in Hilbert space of given dimension d. By choosing $d < |x|$, we prevent Alice from communicating all information about her input x to Bob. There exist distributions obtained from quantum systems of a dimension d that cannot be simulated classically [see, e.g., (27)]. That is, no strategy in which Alice communicates a classical d-valued message to Bob can possibly reproduce the observed data. Such distributions that cannot be classically simulated are candidates for self-testing considerations.

The problem of self-testing consists in characterizing the set of states $\{\rho_x\}$ and/or the set of measurements $\{M_y^b\}$ based only on the distribution $P(b \mid x, y)$. This characterization can usually be done only up to a unitary transformation and possibly a relabeling. In a recent work (28), methods were presented for self-testing sets of pure quantum states and sets of projective measurements in the qubit case. These were subsequently extended to higher dimensional systems in (29, 30).

Formally, a self-test can be made via a witness, which is a linear function of the probability distribution $P(b \mid x, y)$

$$\mathcal{A}[P(b \mid x, y)] = \sum_{x,y,b} \alpha_{xyb} P(b \mid x, y) \tag{3}$$

where α_{xyb} are real coefficients. Moreover, given a witness, one can determine its maximal witness value $\mathcal{A}^Q$ achievable under quantum distributions (Eq. 2) in a bounded Hilbert space. The witness can then be used for self-testing a set of quantum states and/or measurements, whenever there is a unique combination of states and/or measurements that achieves $\mathcal{A}^Q$. Then, it is clear that when the observed distribution $P(b \mid x, y)$ leads to $\mathcal{A}^Q$, a specific set of states and/or measurements is identified (up to a simple class of transformations). A necessary condition for a witness to be useful for self-testing is that, for a given dimension d, quantum systems outperform classical ones; if not, several strategies would generally be compatible with the data [see (21, 21, 27) for examples of such witnesses]. In the "Self-testing nonprojective measurements: Noiseless case" section, we present a method for constructing witnesses whose maximal value can self-test a targeted nonprojective qubit measurement $\mathcal{M}^{\text{target}}$.

Next, we turn to robust self-tests, i.e., self-tests that can be applied even when the statistics is not ideal, causing the witness value to be less than $\mathcal{A}^Q$. This is fundamental to make our methods applicable in practice, as any realistic experiment is prone to noise. The influence of noise makes it impossible to perfectly pinpoint the states and measurements. This motivates the following question. Given an observation of a witness value $\mathcal{A} < \mathcal{A}^Q$, how close are the states and measurements to the ideal ones, i.e., those that would have been perfectly self-tested if we had observed $\mathcal{A} = \mathcal{A}^Q$? In the "Robust self-testing of nonprojective measurements" section, we develop methods for robustly self-testing nonprojective qubit measurements by lower-bounding the fidelity between the implemented measurement and the ideal one. A tight robust self-testing would give the fidelity between the measurement that is most distant from the ideal one and that could have generated a witness value $\mathcal{A} < \mathcal{A}^Q$. Since the presented method does not apply to all types of self-tests, we complement it with a numerical method based on random sampling, which efficiently estimates the robustness of self-testing nonprojective qubit measurements.

Whereas robust self-testing represents a quantitative physical inference, it is also relevant to consider a more qualitative inference. On the basis of the witnesses we develop for self-testing, we show

how to certify that the uncharacterized measurement is nonprojective. In the "Certification methods for nonprojective measurements" section, we determine the largest value of our witness that is compatible with qubit projective measurements. When observing a larger value, the nonprojective character of the measurement is certified. In a similar spirit, we determine a bound on our witness above which a genuine four-outcome (nonprojective) qubit measurement is certified.

An overview of all the self-testing methods developed in this work is illustrated in Fig. 1. The methods will be applied in the "Qubit SIC-POVM" section to self-test particularly relevant non-projective qubit measurements. For these examples, we will demonstrate the usefulness of our methods by implementing them in a photonic experiment. Specifically, our experimental data imply that the implemented measurements are very close to certain ideal three- and four-outcome qubit POVMs and hence are nonprojective. In the latter case, the data certify a genuine four-outcome qubit POVM.

RESULTS

This section presents how to certify and characterize nonprojective measurements in prepare-and-measure scenarios with both noiseless and noisy statistics. The focus will be on qubit systems. Therefore, we begin by summarizing the properties of qubit POVMs.

A POVM with O outcomes is a set of operators $\{E_i\}_{i=1}^{O}$ with the property that $E_i \geq 0$ and that $\sum_i E_i = \mathbb{1}$. In the case of qubits, E_i can be represented on the Bloch sphere as

$$E_i = \lambda_i(\mathbb{1} + \vec{n}_i \cdot \vec{\sigma}) \qquad (4)$$

where $\vec{n}_i$ (with $\vec{n}_i \leq 1$) is the Bloch vector, $\lambda_i \geq 0$, and $\vec{\sigma} = (\sigma_x, \sigma_y, \sigma_z)$ are the Pauli matrices. Positivity and normalization imply that

$$\sum_{i=1}^{O} \lambda_i = 1 \text{ and } \sum_{i=1}^{O} \lambda_i \vec{n}_i = 0 \qquad (5)$$

The set of POVMs is convex, and a POVM is called extremal if it cannot be decomposed as a convex mixture of other POVMs. For qubits, extremal POVMs have either $O = 2,3,4$ outcomes [31]. In the case $O = 2$, extremal POVMs are simply projective, whereas for $O = 3$ and $O = 4$, they are nonprojective; an extremal three-outcome qubit POVM has three unit Bloch vectors in a plane, and an extremal four-outcome qubit POVM has four unit Bloch vectors of which no choice of three are in the same plane [31]. An extremal qubit POVM is therefore characterized by its Bloch vectors. As the statistics of nonextremal POVMs can always be simulated by stochastically implementing extremal POVMs, it is clear that only extremal POVMs can be self-tested.

Self-testing nonprojective measurements: Noiseless case

Consider a target extremal nonprojective qubit POVM $\mathcal{M}^{\text{target}}$, with $O = 3$ or $O = 4$ outcomes, for which we associate the outcome b to the unit Bloch vector $\vec{v}_b$. Our goal is now to construct a witness $\mathcal{A}$ such that its maximal value self-tests $\mathcal{M}^{\text{target}}$. The method consists of two steps summarized in Fig. 2.

Step 1. First, we construct a simpler witness $\mathcal{A}'$ featuring O preparations; i.e., Alice has O inputs. Bob receives an input $y = 1, …, Y$ and provides a binary outcome. The goal of this simpler witness is to self-test a particular relation among the prepared states $|\psi_x\rangle$. Specifically, we would like to certify that their unit Bloch vectors $\vec{u}_x$ point in opposite direction (on the Bloch sphere) to those of the target POVM $\mathcal{M}^{\text{target}}$; i.e., $\vec{u}_x = -\vec{v}_x$ for $x = 1, …, O$. Let us define

$$\mathcal{A}' = \sum_{x,y,b} c_{xyb} P(b \mid x, y) \qquad (6)$$

with real coefficients c_{xyb} chosen such that the maximal value $\mathcal{A}'^Q$ of the witness for qubits self-tests the desired set of prepared states $\{|\psi_x\rangle\}$ (up to a global unitary and relabelings). In general, we believe that it is always possible to find such a self-test by considering enough inputs for Bob, corresponding to well-chosen projective measurements, and suitable coefficients c_{xyb} [see (28) for examples]. Furthermore,
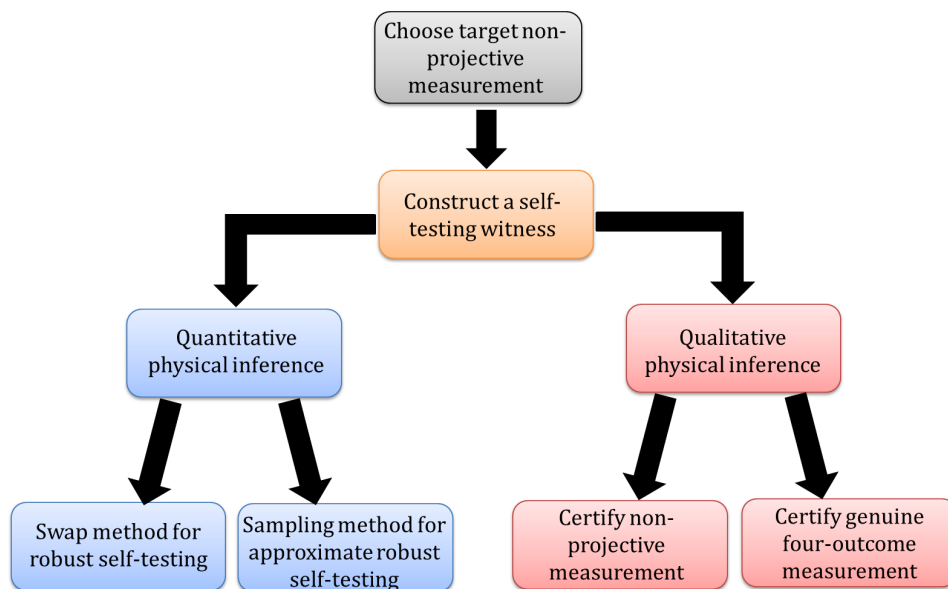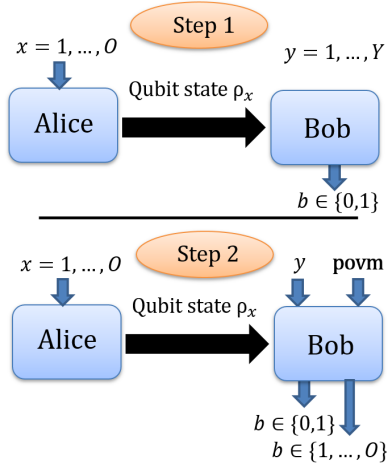

Fig. 1. Graphical overview of the self-testing methods and steps presented in Results.

Fig. 2. Method for self-testing a targeted nonprojective qubit measurement by exploiting simpler self-tests of preparations. Step 1: tailor scenario and witness such that a maximal $\mathcal{A}'$ self-tests Alice's preparations to have Bloch vectors that are anti-aligned with those of the target measurement. Step 2: Add an extra setting to Bob and modify the witness to self-test the target non-projective measurement.

note that one could also, in principle, have more than O preparations for Alice and then self-test that O of them have the desired relation to $\mathcal{M}^{\text{target}}$. In addition, we remark that the construction of an adequate witness $\mathcal{A}'$ is not unique in general.

Step 2. We construct our final witness $\mathcal{A}$ from $\mathcal{A}'$. Specifically, we supply Bob with one additional measurement setting called **povm**. This setting corresponds to a measurement with O outcomes. Since the intention is to self-test the measurement corresponding to this setting as $\mathcal{M}^{\text{target}}$, we associate the setting **povm** to O outcomes. We define

$$\mathcal{A} = \mathcal{A}' - k \sum_{x=1}^{O} P(b = x \mid x, \text{povm}) \tag{7}$$

for some positive constant k. A maximal witness value $\mathcal{A}^Q = \mathcal{A}'^Q$ now implies that the setting **povm** corresponds to $\mathcal{M}^{\text{target}}$ (up to a unitary and relabelings). This is because a maximal witness value implies that (i) the set of prepared states $\{|\psi_x\rangle\}$ have Bloch vectors anti-aligned with those of $\mathcal{M}^{\text{target}}$ and (ii) $P(b = x \mid x, \text{povm}) = 0$ for all x; hence, the Bloch vectors of the setting **povm** are of unit length and aligned with those of $\mathcal{M}^{\text{target}}$. Moreover, as a qubit POVM is characterized by its Bloch vectors, we see that $\mathcal{M}^{\text{target}}$ is the only POVM that can attain the maximal witness value $\mathcal{A}^Q$. Therefore, we obtain a self-test of the target POVM $\mathcal{M}^{\text{target}}$.

In the "Qubit SIC-POVM" section, we will apply this method to self-test symmetric qubit POVMs with three and four outcomes.

Robust self-testing of nonprojective measurements
No experiment can achieve the noiseless conditions needed to obtain exactly a maximal value of $\mathcal{A}$. Therefore, it is paramount to discuss the case when a nonmaximal value of $\mathcal{A}$ is observed. We will show that, in this case, one can nevertheless make a statement about how close the uncharacterized measurement $\mathcal{E}$ performed in the laboratory (corresponding to the setting **povm**) is to the target POVM $\mathcal{M}^{\text{target}}$.

To address this question, we must first define a measure of closeness between two measurements. A natural and frequently used dis-

tance measure in quantum information is the fidelity, F, between two operators. We consider a measure of closeness amounting to the best possible weighted average fidelity between the extremal qubit target POVM elements $M^{\text{target}} = \{M_i\}$ and the actual POVM elements $\mathcal{E} = \{E_i\}$. That is, we allow for a quantum extraction channel Λ to be applied to the actual POVM. The set of allowed extraction channels is the set of unital channels in the relevant Hilbert space dimension. This is understood from the fact that the extraction channel must map O-outcome POVMs to O-outcome POVMs in the given Hilbert space dimension. Because of linearity, this implies that the channel is unital. Conversely, since every channel preserves positivity, every unital channel in the relevant Hilbert space dimension maps POVMs to POVMs. We look for the best possible extraction channel. We thus define the quantity

$$F(E, M^{\text{target}}) = \max_{\Lambda} \frac{1}{2} \sum_{i=1}^{O} \frac{tr\,(\Lambda\,[\,E_i]\,M_i)}{tr\,(M_i)} \tag{8}$$

Since the target measurement is extremal, the POVM elements are proportional to rank-one projectors; $M_i \propto P_i$. Because of Eq. 4, we can write $\Lambda[E_i] = \lambda_i(\mathbb{1} + \vec{n}_i \cdot \vec{\sigma})$ subject to the constraints (Eq. 5). By evaluating Eq. 8, we find that $F = 1/2 + 1/2 \sum_i \lambda_i \text{tr}\,(P_i \vec{n}_i \cdot \vec{\sigma}_i) \leq 1$. To saturate the inequality, each Bloch vector $\vec{n}_i$ must be of unit length, i.e., $|\vec{n}_i| = 1$, and aligned with the Bloch vector of P_i. Hence, M_i and $\Lambda[E_i]$ are both proportional to the same rank-one projector. Since a POVM with Bloch vectors of unit length is fully characterized, i.e., all coefficients λ_i are fixed by the conditions (Eq. 5), this implies that $M_i = \Lambda[E_i]$. Thus, a maximal fidelity of $F = 1$ is uniquely achieved when the actual POVM is equal to the target measurement.

In general, a nonmaximal value of the witness $\mathcal{A}$ can arise from many different possible choices of states and measurements. We denote by $S(\mathcal{A})$ the set of all O-outcome POVMs that are compatible with a given observed value $\mathcal{A}$. Our goal is now to find a lower-bound on the average fidelity F that holds for every measurement $\mathcal{E} \in S(\mathcal{A})$. Therefore, the quantity of interest is the worst-case average fidelity:

$$\mathcal{F}(\mathcal{A}) = \min_{\mathcal{E} \in S(\mathcal{A})} F(\mathcal{E}', \mathcal{M}^{\text{target}}) \tag{9}$$

Calculating this quantity, or even lower-bounding it, is typically a nontrivial problem even in the simplest case. We proceed with presenting two methods for this task.

We remark that the definition (Eq. 8), given for qubits, could potentially be extended to higher-dimensional systems (replacing the factor 1/2 by 1/d). This could work for POVMs where all elements are proportional to rank-one projectors. However, the latter are only a strict subset of general extremal POVMs. Finding a more general figure of merit is thus an interesting open question.

Robust self-testing with the swap method
A lower-bound on the worst-case average fidelity can be obtained via semidefinite programming (32). The method combines the so-called swap method (33, 34), introduced for self-testing in the Bell scenario, and the hierarchy of dimensionally bounded quantum correlations (35). Such adaptations of the swap method to prepare-and-measure scenarios were introduced in (28) to self-test pure state and projective measurements. In section S1, we outline the details of how the swap method is adapted to robustly self-test nonprojective measurements. This method benefits from being applicable in a variety of scenarios and for returning rigorous lower bounds on $\mathcal{F}$. Nevertheless, it suffers from two drawbacks. First, the method only overcomes the fact that self-tests are valid up to a global unitary, but

not that they may be valid up to relabelings. Thus, it is only useful for target measurements that are self-tested up to a unitary. Second, while rarely producing tight bounds on $\mathcal{F}$, the computational requirements scale rapidly with the number of inputs, the number of outputs, and the chosen level of the hierarchy. In the "Qubit SIC-POVM" section, we will show that the method can be efficiently applied for robustly self-testing a three-outcome qubit POVM.

Numerically approximating robust self-testing

To also address cases in which self-tests are valid up to both a unitary transformation and relabelings, we can estimate $\mathcal{F}$ based on random sampling. The approximation method benefits from being straightforward and broadly useful, while it suffers from the fact that it merely estimates the value of $\mathcal{F}$ instead of providing a strict lower bound. The key feature is that the minimization appearing in Eq. 9 is replaced by a minimization taken over data obtained from many random samples of the setting **povm**. We detail this method in section S2 and apply it to an example in the "Qubit SIC-POVM" section.

Certification methods for nonprojective measurements

Whereas robust self-testing considers quantitative aspects of physical inference from noisy data, it is important to also consider the qualitative inference. An important qualitative statement is to prove that the uncharacterized measurement is nonprojective or, more generally, that it cannot be simulated by projective measurements. It is known that when POVMs are sufficiently noisy, they become perfectly simulable via projective measurements (19, 36, 37). The witnesses we construct can address this question. We will see that whenever the observed value of the witness $\mathcal{A}$ is sufficiently large, one can certify that the setting **povm** necessarily corresponds to some nonprojective measurement and could not have been simulated via projective measurements. Specifically, we derive an upper bound on $\mathcal{A}$ for projective measurements (or convex combination of them). The violation of such a bound thus certifies a nonprojective measurement or, more precisely, a genuine three-outcome (or four-outcome) POVM. At the end of this subsection, we also show how to certify a genuine four-outcome POVM.

A projective qubit measurement has binary outcomes and can therefore be represented by an observable $M \equiv M_0 - M_1$, where M_i is the measurement operator corresponding to outcome $i = 0,1$. Let us consider the case where the O-outcome measurement **povm** is projective. One may assign two outcomes to rank-one projectors and the rest to trivial zero operators. Note that it is enough here to consider these cases, as the witness $\mathcal{A}$ is linear in terms of the measurement operators. Projectors can thus be assigned in three ($O = 3$) or six ($O = 4$) different ways, of which the optimal instance must be chosen. Let the outcomes in the optimal instance be $o_{0|\text{povm}}$ and $o_{1|\text{povm}}$ and associate the observable $M_{\text{povm}} \equiv M_{Y+1} = M_{\text{povm}}^{o_{0|\text{povm}}} - M_{\text{povm}}^{o_{1|\text{povm}}}$. The witness (Eq. 7) can be written as

$$\mathcal{A} = C(k) + \sum_x \text{tr}[\rho_x \mathcal{L}_x^{(k)}(\{M_y\})] \tag{10}$$

where $C(k)$ is a constant and $\mathcal{L}_x^{(k)}(\{M_y\})$ is a linear combination of the observables $\{M_1, \ldots, M_{Y+1}\}$. Note that $\mathcal{L}_x^{(k)}(\{M_y\})$ does not depend on the index y but on the collection of observables. Using the Cauchy-Schwarz inequality for operators, we obtain

$$\mathcal{A} \leq C(k) + \sum_x \sqrt{\text{tr}[\rho_x \mathcal{L}_x^{(k)}(\{M_y\})^2]} \tag{11}$$

Because of projectivity, we have $M_y = \vec{n}_y \cdot \vec{\sigma}$, where $\vec{n}_y$ is of unit length. Using $\{M_k, M_l\} = 2\vec{n}_k \cdot \vec{n}_l \mathbb{1}$, one finds $\mathcal{L}_x^{(k)}(\{M_y\})^2 = t_x^{(k)}(\{\vec{n}_y\})\mathbb{1}$, for some function t, which is a weighted sum of scalar products of the Bloch vectors of the observables. Consequently, to bound $\mathcal{A}$ under all projective measurements, we have

$$\mathcal{A} \overset{\text{Proj}}{\leq} C(k) + \max_{\{\vec{n}_y\}} \sum_x \sqrt{t_x^{(k)}(\{\vec{n}_y\})} \equiv \mathcal{B}(k) \tag{12}$$

Thus, $\mathcal{B}(k)$ bounds the value of $\mathcal{A}$ for projective measurements. The evaluation of this bound only depends on Bob's Bloch vectors and is further simplified by their parameterization in terms of two angles. The effort needed to evaluate the bound depends on the chosen prepare-and-measure scenario. Typically, considering scenarios with some symmetry properties is beneficial.

Moreover, when targeting a four-outcome qubit POVM, we consider also a finer form of qualitative characterization by considering whether $\mathcal{A}$ can be simulated by the setting **povm** being some three-outcome POVM. If not, the measurement is certified as a genuine four-outcome measurement. This amounts to bounding the value of $\mathcal{A}$ achievable under any two- or three-outcome qubit POVM and then observing a violation of that bound. For this purpose, one may use the hierarchy of dimensionally bounded quantum correlations (35), which can be used to upper-bound $\mathcal{A}$ under three-outcome POVMs. Since the hierarchy is built on projective measurements, one must embed Alice's preparations in a larger Hilbert space with the dimension chosen such that three-outcome POVMs can be recast as projective measurement following Neumark's theorem. To obtain tight bounds, one may need a reasonably high hierarchy level, which can be efficiently implemented using the methods of (30).

Next, in the "Qubit SIC-POVM" section, we will apply the outlined methods to specific nonprojective measurements and experimentally demonstrate the certification of both nonprojective and genuine four-outcome measurements.

Relevant examples and their experimental realization

In the above, we have discussed methods for self-testing a target nonprojective measurement. Here, we put these methods in practice in a photonic experiment. We implement three- and four-outcome symmetric qubit POVMs, with Bloch vectors forming a star (trine-POVM) and a tetrahedron (SIC-POVM), respectively. In the first case, we certify a nonprojective measurement and apply our methods for robust self-testing, demonstrating worst-case average fidelity of at least 96% compared to an ideal trine-POVM. In the second case, we certify a genuine four-outcome qubit POVM and demonstrate worst-case average fidelity of approximately 98% with respect to an ideal SIC-POVM. We consider each example separately by first applying the methods of Results to obtain adequate witnesses and then present the corresponding experimental realization. The setup common to both experiments is presented in Materials and Methods.

Qubit SIC-POVM

We begin by illustrating the self-testing methods for a frequently used nonprojective measurement, namely, the qubit SIC-POVM, which we denote $\mathcal{M}_{\text{SIC}}$. This measurement has four outcomes, and its four unit Bloch vectors $\{\vec{v}_b\}_b$ form a regular tetrahedron on the Bloch sphere, with weights $\lambda_b = 1/4$. Such a regular tetrahedron construction can be achieved via two different labelings of the four outcomes that are not equivalent under unitary transformations.

Up to a unitary transformation, each such SIC-POVM can be written with Bloch vectors

$$\vec{v}_1 = [1,1,1]/\sqrt{3} \qquad \vec{v}_2 = [1,-1,-1]/\sqrt{3}$$
$$\vec{v}_3 = [-1,1,-1]/\sqrt{3} \qquad \vec{v}_4 = [-1,-1,1]/\sqrt{3} \qquad (13)$$

and the set of Bloch vectors $\{-\vec{v}_l\}_l$, respectively.

Noiseless self-test

We find a prepare-and-measure scenario for self-testing $\mathcal{M}_{SIC}$. Following step 1 in the "Self-testing nonprojective measurements: Noiseless case" section, we introduce a prepare-and-measure scenario in which Alice has four preparations, $x \in \{1,2,3,4\}$, and Bob has three binary-outcome measurements, $y \in \{1,2,3\}$. The witness is chosen as

$$\mathcal{A}'_{SIC} = \frac{1}{12}\sum_{x,y} P(b = S_{x,y} | x,y) \qquad (14)$$

where $S_{1,y} = [0,0,0]$, $S_{2,y} = [0,1,1]$, $S_{3,y} = [1,0,1]$, and $S_{4,y} = [1,1,0]$. The maximal value, $\mathcal{A}'_{SIC} = 1/2(1 + 1/\sqrt{3})$, can be achieved by Alice preparing her four states forming a regular tetrahedron, e.g., with the Bloch vectors in Eq. 13, and Bob performing the measurements σ_x, σ_y, and σ_z. In section S3, we prove the maximal witness value and show that it self-tests that Alice's preparations indeed must form a regular tetrahedron on the Bloch sphere. By step 2 in the "Self-testing nonprojective measurements: Noiseless case" section, we supply Bob with an additional four-outcome measurement **povm** and consider the modified witness

$$\mathcal{A}_{SIC} = \frac{1}{12}\sum_{x,y} P(b = S_{x,y} | x,y) - k\sum_{x=1}^{4} P(b = x | x, \textbf{povm}) \qquad (15)$$

Thus, we conclude that $\mathcal{A}_{SIC} = 1/2(1 + 1/\sqrt{3})$ self-tests $\mathcal{M}_{SIC}$.

We note that there also exist other prepare-and-measure scenarios fulfilling the requirements of step 1. For example, one may achieve the desired self-test using the so-called $3 \to 1$ random access code whose self-testing properties were considered in (28). However, this prepare-and-measure scenario requires more preparations than the one presented here.

Robust self-test

Next, we consider the worst-case fidelity (given in Eq. 9) of the measurement corresponding to the setting **povm** with $\mathcal{M}_{SIC}$. Since the self-test of $\mathcal{M}_{SIC}$ is valid up to a relabeling and a collective unitary, we cannot use the swap method to lower-bound $\mathcal{F}$. Instead, we use the numerical approximation method (see section S2 for details). Figure 3 displays roughly 3×10^5 optimal pairs $(\mathcal{A}_{SIC}, F)$ each evaluated from a randomly sampled measurement for the setting **povm**. The evaluation was done for $k = 1/5$ (which, as will soon be shown, turns out to be the most noise-resilient choice of k). We see that the minimal sampled fidelity as a function of $\mathcal{A}_{SIC}$ describes a curve, which constitutes the approximation of $\mathcal{F}$.

Certifying nonprojective and genuine four-outcome POVMs

Last, we derive a tight bound valid for all qubit projective measurements on the value of $\mathcal{A}_{SIC}$. Because of the symmetries of $\mathcal{A}_{SIC}$, we can, without loss of generality, let the nontrivial (nonzero measurement operator) outcomes of the measurement **povm** be the outcomes $b = 1,2$. Hence, we define the observable $M_{\textbf{povm}} \equiv M_4 = M_{\textbf{povm}}^1 - M_{\textbf{povm}}^2$. Then, we follow the steps outlined in the "Certification methods for nonprojective measurements" section. First, we re-write $\mathcal{A}_{SIC}$ in the form of Eq. 10. We find $C(k) = (1 - 2k)/2$ and
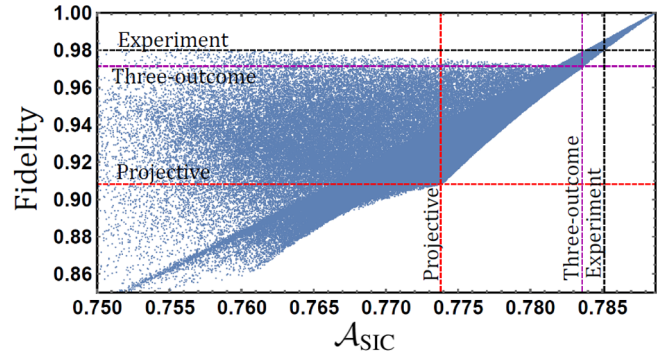
Fig. 3. Numerical approximation of the worst-case fidelity of the unknown measurement (setting povm) with the qubit SIC-POVM by roughly 3×10⁵ random three- and four-outcome POVM samples for which the optimal values of $(\mathcal{A}, \mathcal{F})$ were calculated. The figure also displays the critical limits on $\mathcal{A}_{SIC}$ and $\mathcal{F}$ for projective and three-outcome POVMs, respectively, as well as the experimentally measured values.

$$\mathcal{L}_{x=0,1}^{(k)}(\{M_y\}) = \frac{1}{24}[1, (-1)^x, (-1)^x, (-1)^{x+1} 12k]\cdot\vec{M}$$
$$\mathcal{L}_{x=2,3}^{(k)}(\{M_y\}) = \frac{1}{24}[-1, (-1)^x, (-1)^{x+1}, 0]\cdot\vec{M} \qquad (16)$$

where $\vec{M} = [M_1, M_2, M_3, M_4]$, with $M_y = \vec{n}_y \cdot \vec{\sigma}$. After applying the Cauchy-Schwarz inequality, we obtain a cumbersome expression of the form of Eq. 11. To evaluate its maximal value (following Eq. 12), we use the following concavity inequality: $\sqrt{r} + \sqrt{s} \leq \sqrt{2(r+s)}$ for $r, s \geq 0$, with equality if and only if $r = s$. Apply this inequality twice to the expression (Eq. 12), first to the two terms associated to $x = 0,1$, and then to the two terms associated to $x = 2,3$. After a simple optimization over $\vec{n}_3$ and denoting $x = \vec{n}_1 \cdot \vec{n}_2$, one arrives at

$$\mathcal{A}_{SIC} \leq \frac{1-2k}{2} + \frac{\sqrt{2}}{24}\sqrt{6-4x}$$
$$+ \frac{\sqrt{2}}{24}\sqrt{2r_k + 4x + 48k\sqrt{2}\sqrt{1+x}} \equiv f_k(x)$$

where $r_k = 3 + 144k^2$. This bound is valid for a particular value of x. To hold for all projective measurements, we simply maximize $f_k(x)$ over x. This requires only an optimization in a single real variable $x \in [-1,1]$, which is straightforward. The optimal choice is denoted x^*. Setting $\mathcal{B}(k) = f_k(x^*)$, we have $\mathcal{A}_{SIC} \leq \mathcal{B}(k)$ for all projective measurements. Although the expressions involved are cumbersome, the analysis is simple and straightforward. We have considered the tightness of the projective bound for $k \in \{1/100, 2/100, \dots, 1\}$ by numerically optimizing $\mathcal{A}_{SIC}$ under unit-trace measurements (which includes all rank-one projective measurements). In all cases, we saturate the bound $\mathcal{B}(k)$ up to machine precision with a projective measurement.

Furthermore, we have also considered bounding $\mathcal{A}_{SIC}$ under three-outcome qubit POVMs using the hierarchy of dimensionally bounded quantum correlations (as described in the "Certification methods for nonprojective measurements" section). In our implementation of (35), we have embedded the qubit preparations into a three-dimensional Hilbert space and optimized $\mathcal{A}_{SIC}$ under projective measurements of the only existing nontrivial rank combination. The relaxation level involved some monomials from both the second and third level, and the size of the moment matrix was 126. This was

done for all $k \in \{1/100, 2/100 \dots, 1\}$, and each upper bound was saturated up to numerical precision using lower bounds numerically obtained via semidefinite programs.

To study the robustness of both the nonprojective and the genuine four-outcome certification, we have considered the critical visibility of the system needed when exposed to noise. This is modeled by the preparations taking the form $\rho_x(v) = v\rho_x + (1 - v)\rho_{\text{noise}}$, where $v \in [0,1]$ is the visibility and ρ_{noise} is some arbitrary qubit state. A straightforward calculation shows that the critical visibility for violating some given bound $\mathcal{B}$ is

$$v_{\text{crit}}(k) = \frac{\mathcal{B}(k) - \mathcal{A}^{\text{rand}} + k}{\mathcal{A}^{Q} - \mathcal{A}^{\text{rand}} + k} \qquad (17)$$

where $\mathcal{A}^{\text{rand}}$ is the witness value obtained from the optimal measurements performed on the maximally mixed state. Notably, this expression is independent of the specific form of ρ_{noise}. We have applied this to $\mathcal{A}_{\text{SIC}}$ with $\mathcal{B}(k)$, corresponding to the bounds on projective and three-outcome measurements, respectively. The corresponding critical visibilities are plotted in section S5. In both cases, we find that the largest amount of noise is tolerated for $k = 1/5$, corresponding to $v_{\text{crit}} = 0.970$ and $v_{\text{crit}} = 0.990$, respectively.

Experimental result
Wave-plate settings for Alice's prepared states in Eq. 13 and Bob's measurements σ_x, σ_y, σ_z, and the four-outcome SIC-POVM anti-aligned to the vectors in Eq. 13, are reported in section S5. In section S5, we also report a state tomography of Alice's preparations.

Optimally choosing $k = 1/5$, the measured value of the witness as compared to the relevant bounds is

$$A_{\text{SIC}} \overset{\text{projective}}{\leq} 0.7738 \overset{\text{3-outcome}}{\leq} 0.7836 \overset{\text{qubit}}{\leq} 0.7887. \qquad (18)$$
$$A_{\text{SIC}}^{\text{Lab}} = 0.78514 \pm 5 \times 10^{-5}_{\text{stat}} \pm 1.0 \times 10^{-4}_{\text{syst}}$$

The statistical error originates from Poissonian statistics, and the systematic error originates from the precision of the wave-plate settings. More details about the errors are discussed in section S5.

We observe a substantial violation of both the projective measurement and the three-outcome measurement bounds. Thus, we can certify that Bob's measurement **povm** is a genuine four-outcome qubit POVM. Furthermore, as illustrated by the results in Fig. 3, we certify approximately a 98% worst-case fidelity with the qubit SIC-POVM.

Qubit trine-POVM
We consider a second example in which the target POVM is the so-called trine-POVM. This measurement has three outcomes, and its Bloch vectors form an equilateral triangle on a disk of the Bloch sphere, with $\lambda_l = 1/3$. The Bloch vectors are hence defined by

$$\vec{v}_1 = [0, 0, -1], \quad \vec{v}_2 = \frac{1}{2}[-\sqrt{3}, 0, 1], \quad \vec{v}_3 = \frac{1}{2}[\sqrt{3}, 0, 1] \qquad (19)$$

Noiseless self-test
We introduce a prepare-and-measure scenario in which Alice has three inputs $x \in \{1,2,3\}$, and Bob has two binary-outcome measurements labeled by $y \in \{1,2\}$, and consider the witness

$$\mathcal{A}'_{\text{tri}} = \sum_{x,y,b} T_{x,y} (-1)^b P(b \mid x, y) \qquad (20)$$

where $T_{x,1} = [1, 1, -1]$ and $T_{x,2} = [\sqrt{3}, -\sqrt{3}, 0]$. In section S3, we show that its maximal value is $\mathcal{A}'_{\text{tri}} = 5$, and that this value implies that Alice's three preparations form an equilateral triangle on the Bloch

sphere. Then, we add an additional input **povm** for Bob and consider the witness

$$\mathcal{A}_{\text{tri}} = \sum_{x,y,b} T_{x,y} (-1)^b P(b \mid x, y) - k \sum_{x=1}^{3} P(b = x \mid x, \textbf{povm}) \qquad (21)$$

for some $k > 0$. Then, $\mathcal{A}_{\text{tri}} = 5$ self-tests the setting **povm** as the trine-POVM up to a unitary.

Robust self-test
We now turn to considering its robust self-testing properties, i.e., lower-bounding the worst-case fidelity of the unknown measurement (setting **povm**) with the target measurement for a given value of $\mathcal{A}_{\text{tri}}$. Since the above self-test is achieved only up to unitary transformations, we may find rigorous lower bounds on the worst-case fidelity $\mathcal{F}$ using semidefinite programming. In accordance with the "Robust self-testing of nonprojective measurements" section, we have performed the swap-operation on Bob's side and used the hierarchy of finite-dimensional correlations to lower-bound $\mathcal{F}$. The hierarchy level was an intermediate level containing some higher-order moments corresponding to an SDP matrix of size 105. In addition, for the sake of comparison, we have implemented the numerical approximation method for robust self-testing to estimate the accuracy of the bound obtained via the swap method. The results are shown in Fig. 4. A comparison suggests that the swap method returns a suboptimal bound. Its accuracy could potentially be improved by using a higher hierarchy level. Nevertheless, the obtained bound will prove sufficient for the practical purpose of experimentally certifying the targeted POVM with high accuracy.

Last, we have also self-tested the trine-POVM in a different prepare-and-measure scenario (see section S3). In section S4, we use this prepare-and-measure scenario to derive a tight bound on projective measurements by evaluating the right-hand side of Eq. 12.

Experimental realization
The witness in Eq. 21 is maximized if Alice's three Bloch vectors point to the vertices of an equilateral triangle on a disk of the Bloch sphere. We take that disk to be the xz plane, taking $\vec{t}_i = -\vec{v}_i$ (from Eq. 19), and Bob performs one of three measurements σ_z, σ_x, and the three-outcome POVM with vectors anti-aligned to Alice's states. See section S5 for state tomography of Alice's preparations. In contrast to the previous experiment, output 2 of Bob's measurement station only consists of one detector (D3) and no wave plate or polarizing beamsplitter (PBS) (see Fig. 5). The wave-plate settings corresponding to the above states and measurements are reported in section S5.
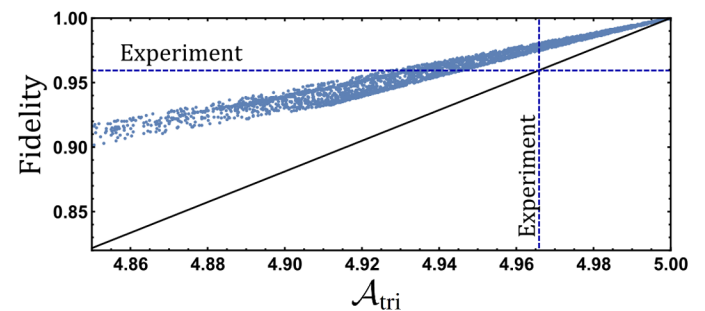
Fig. 4. Lower bound on $\mathcal{F}(\mathcal{A}_{\textbf{tri}})$ for k=1 obtained from the swap method, together with roughly 3000 points $(\mathcal{A}_{\textbf{tri}}, \mathcal{F})$ obtained via the numerical approximation method. This is displayed next to the experimentally achieved results.
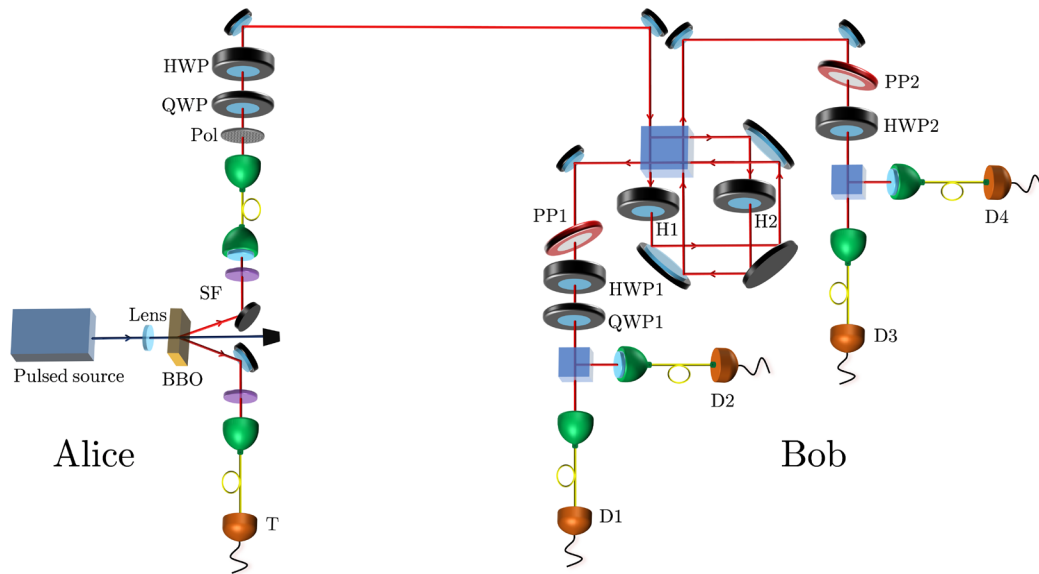
Fig. 5. Experimental setup. More details, including labeling, can be found in the main text. Pol, polarizer.

With the said settings, we have obtained the experimentally measured value of $\mathcal{A}_{\text{tri}}$ as a function of k. Since we aim to demonstrate a large worst-case fidelity with the trine-POVM, we have computed the lower bound on $\mathcal{F}(\mathcal{A}_{\text{tri}})$ for many different values of k and found that choosing $k = 1$ leads to the optimal result. The corresponding experimentally measured witness is

$$\mathcal{A}_{\text{tri}}(k = 1) \overset{\text{projective}}{\leq} 4.89165 \overset{\text{qubit}}{\leq} 5 \qquad (22)$$

$$\mathcal{A}_{\text{tri}}^{\text{Lab}}(k = 1) = 4.9659 \pm 7 \times 10^{-4}_{\text{stat}} \pm 1.7 \times 10^{-3}_{\text{syst}} \qquad (23)$$

This data point and its relation to the worst-case fidelity of the laboratory measurement with the targeted POVM are depicted in Fig. 4. From $\mathcal{A}_{\text{tri}}^{\text{Lab}}$, we infer a closeness of at least 96%. This can be compared to the largest possible fidelity between a projective measurement and the trine-POVM, which is straightforwardly found to be $(2 + \sqrt{3})/4 \approx 0.933$. However, as indicated by the results of the sampling-based numerical approximation method for robust self-testing (presented in Fig. 4), a better bound of $\mathcal{F}$ may allow us to rigorously infer a worst-case fidelity of at least 97.3%.

Furthermore, we have considered the possibility of the experimental data certifying a nonprojective qubit measurement. However, to this end, we found that another choice of k is optimal with respect to the witness value that is achievable under projective measurements. We found that the optimal choice is $k \approx 4.5$. The corresponding experimentally measured value becomes

$$\mathcal{A}_{\text{tri}}(k = 4.5) \overset{\text{projective}}{\leq} 4.71139 \overset{\text{qubit}}{\leq} 5 \qquad (24)$$
$$\mathcal{A}_{\text{tri}}^{\text{Lab}}(k = 4.5) = 4.93613 \pm 5 \times 10^{-5}_{\text{stat}} \pm 1.0 \times 10^{-4}_{\text{syst}}$$

We conclude that our experimental data certifies a nonprojective qubit measurement.

DISCUSSION

We investigated the problem of self-testing nonprojective measurements. We argued that a prepare-and-measure scenario with an upper bound on the Hilbert space dimension represents a natural framework for investigating this problem. We considered both the qualitative certification of a measurement being nonprojective and/or genuine four-outcome, as well as a quantitative characterization in terms of worst-case fidelity to a given target POVM. We demonstrate the practical relevance of these methods in two experiments in which we both certify a genuine four-outcome POVM and infer a high worst-case fidelity with respect to target symmetric qubit POVMs.

It would be interesting to overcome the limitation of the swap method and develop a rigorous robust self-testing method for general four-outcome qubit POVMs. Also extending these methods to high-dimensional POVMs would be relevant since there exist extremal nonprojective measurements that feature the same number of outcomes as projective measurements (contrary to the qubit case). Moreover, it would be interesting to investigate self-testing of nonprojective measurements using different assumptions as in our work. One could consider for instance prepare-and-measure scenarios with a bound on the entropy (38), the overlap between the prepared states (8), or their mean energy (39). Last, one may ask whether it would be possible to robustly self-test a nonprojective measurement in the fully device-independent case, i.e., returning to the Bell scenario without any assumption on the dimension.

MATERIALS AND METHODS

In the experiment, the qubit states are encoded in the polarization degree of freedom of a single photon, with the convention of $|H\rangle \equiv |0\rangle$ and $|V\rangle \equiv |1\rangle$. The setup is depicted in Fig. 5.

Alice's station includes a heralded single-photon source where femtosecond laser pulses at 390 nm are converted into pairs of photons at 780 nm, through type I spontaneous parametric down-conversion in two orthogonally oriented beta-barium borate crystals. Photon

pairs go through 3-nm spectral filters and are then coupled into two single-mode fibers for spatial mode filtering. The idler photon is sent to the trigger avalanche photodiode (APD) detector (T) and heralds the presence of a signal photon. The latter is then emitted again into free space and undergoes Alice's state preparation, consisting of a fixed linear polarizer, a $\lambda/4$ wave plate [or quarter–wave plate (QWP)], and a $\lambda/2$ wave plate [or half–wave plate (HWP)].

Upon preparing the required qubit state, Alice forwards the signal photon to Bob's measurement station, where it goes through a double-path Sagnac interferometer, each path of which contains an HWP. The interferometer mixes the polarization degree of freedom with path, effectively enabling Bob to perform either projective or nonprojective measurements in the original polarization Hilbert space where the qubit was prepared, thanks to the two polarization analyzers at the outputs. Each of these consists of a phase plate, an HWP, and (in output 1) a QWP, a polarizing beam splitter and two single-photon detectors. Outputs from all detectors (T and D1 to D4) are sent to a coincidence unit connected to a computer.

All measurements were performed with heralded photon rates of approximately 1×10^4 counts per second, while each setting was measured for 500 s. We have made an assumption of fair sampling, i.e., that the detection events are representative of the total number of signal photons. This assumption is reasonable for tasks that do not include a notion of an adversary. The quality of state preparation and measurement can be estimated by preparing states $|H\rangle$, $|+\rangle = (|H\rangle + |V\rangle)/\sqrt{2}$, and $|R\rangle = (|H\rangle + i\,|V\rangle)/\sqrt{2}$ and measuring them in the Pauli bases σ_z, σ_x, and σ_y, respectively. The three visibilities obtained in our setup with this characterization measurement were

$$
\begin{aligned}
V_{\sigma_z} &= (99.91 \pm 0.02)\,\% \\
V_{\sigma_x} &= (99.31 \pm 0.01)\,\% \\
V_{\sigma_y} &= (99.23 \pm 0.02)\,\%
\end{aligned}
\tag{25}
$$

While the almost optimal V_{σ_z} is a direct consequence of the high extinction ratios of the PBSs used, the lower visibilities in the interference bases are mainly due to the double-path Sagnac interferometer, which showed a visibility of around 99.4%, therefore effectively bounding from above the results we can achieve in the experiments.

Note added. During the completion of this manuscript, we became aware of an independent work (*40*) discussing the certification of qubit POVMs.

SUPPLEMENTARY MATERIALS

Supplementary material for this article is available at http://advances.sciencemag.org/cgi/content/full/6/16/eaaw6664/DC1

REFERENCES AND NOTES

1. R. Derka, V. Bužek, A. K. Ekert, Universal algorithm for optimal estimation of quantum states from finite ensembles via realizable generalized measurement. *Phys. Rev. Lett.* **80**, 1571–1575 (1998).
2. J. M. Renes, R. Blume-Kohout, A. J. Scott, C. M. Caves, Symmetric informationally complete quantum measurements. *J. Math. Phys.* **45**, 2171–2180 (2004).
3. J. Shang, A. Asadian, H. Zhu, O. Gühne, Enhanced entanglement criterion via symmetric informationally complete measurements. *Phys. Rev. A* **98**, 022309 (2018).
4. D. Dieks, Overlap and distinguishability of quantum states. *Phys. Lett. A* **126**, 303–306 (1988).
5. A. Peres, How to differentiate between non-orthogonal states. *Phys. Lett. A* **128**, 19 (1988).
6. C. H. Bennett, Quantum cryptography using any two nonorthogonal states. *Phys. Rev. Lett.* **68**, 3121–3124 (1992).
7. J. M. Renes, Spherical-code key-distribution protocols for qubits. *Phys. Rev. A* **70**, 052314 (2004).
8. J. B. Brask, A. Martin, W. Esposito, R. Houlmann, J. Bowles, H. Zbinden, N. Brunner, Megahertz-rate semi-device-independent quantum random number generators based on unambiguous state discrimination. *Phys. Rev. Appl.* **7**, 054018 (2017).
9. T. Vértesi, E. Bene, Two-qubit Bell inequality for which positive operator-valued measurements are relevant. *Phys. Rev. A* **82**, 062115 (2010).
10. A. Acín, S. Pironio, T. Vértesi, P. Wittek, Optimal randomness certification from one entangled bit. *Phys. Rev. A* **93**, 040102 (2016).
11. S. Gómez, A. Mattar, E. S. Gómez, D. Cavalcanti, O. Jiménez Farías, A. Acín, G. Lima, Experimental nonlocality-based randomness generation with non-projective measurements. *Phys. Rev. A* **97**, 040102 (2018).
12. D. Mayers, A. Yao, Self testing quantum apparatus. *Quantum Inform. Comput.* **4**, 273–286 (2004).
13. J. F. Clauser, M. A. Horne, A. Shimony, R. A. Holt, Proposed experiment to test local hidden-variable theories. *Phys. Rev. Lett.* **23**, 880–884 (1969).
14. S. J. Summers, R. Werner, Bell's inequalities and quantum field theory. II. Bell's inequalities are maximally violated in the vacuum. *J. Math. Phys.* **28**, 2448–2456 (1987).
15. S. Popescu, D. Rohrlich, Which states violate Bell's inequality maximally? *Phys. Lett. A* **169**, 411–414 (1992).
16. B. S. Tsirelson, Some results and problems on quantum Bell-type inequalities. *Hadronic J. Suppl.* **8**, 329–345 (1993).
17. M. McKague, T. H. Yang, V. Scarani, Robust self-testing of the singlet. *J. Phys. A Math. Theor.* **45**, 455304 (2012).
18. B. W. Reichardt, F. Unger, U. Vazirani, Classical command of quantum systems. *Nature* **496**, 456–460 (2013).
19. M. Oszmaniec, L. Guerini, P. Wittek, A. Acín, Simulating positive-operator-valued measures with projective measurements. *Phys. Rev. Lett.* **119**, 190501 (2017).
20. E. S. Gómez, S. Gómez, P. González, G. Cañas, J. F. Barra, A. Delgado, G. B. Xavier, A. Cabello, M. Kleinmann, T. Vértesi, G. Lima, Device-independent certification of a nonprojective qubit measurement. *Phys. Rev. Lett.* **117**, 260401 (2016).
21. M. Hendrych, R. Gallego, M. Mičuda, N. Brunner, A. Acín, J. P. Torres, Experimental estimation of the dimension of classical and quantum systems. *Nat. Phys.* **8**, 588–591 (2012).
22. J. Ahrens, P. Badziąg, A. Cabello, M. Bourennane, Experimental device-independent tests of classical and quantum dimensions. *Nat. Phys.* **8**, 592–595 (2012).
23. M. Smania, A. M. Elhassan, A. Tavakoli, M. Bourennane, Experimental quantum multiparty communication protocols. *npj Quant. Inf.* **2**, 16010 (2016).
24. T. Lunghi, J. B. Brask, C. C. W. Lim, Q. Lavigne, J. Bowles, A. Martin, H. Zbinden, N. Brunner, Self-testing quantum random number generator. *Phys. Rev. Lett.* **114**, 150501 (2015).
25. A. Tavakoli, A. Hameedi, B. Marques, M. Bourennane, Quantum random access codes using single *d*-level systems. *Phys. Rev. Lett.* **114**, 170502 (2015).
26. D. Martínez, A. Tavakoli, M. Casanova, G. Cañas, B. Marques, G. Lima, High-dimensional quantum communication complexity beyond strategies based on Bell's theorem. *Phys. Rev. Lett.* **121**, 150504 (2018).
27. R. Gallego, N. Brunner, C. Hadley, A. Acín, Device-independent tests of classical and quantum dimensions. *Phys. Rev. Lett.* **105**, 230501 (2010).
28. A. Tavakoli, J. Kaniewski, T. Vértesi, D. Rosset, N. Brunner, Self-testing quantum states and measurements in the prepare-and-measure scenario. *Phys. Rev. A* **98**, 062307 (2018).
29. M. Farkas, J. Kaniewski, Self-testing mutually unbiased bases in the prepare-and-measure scenario. *Phys. Rev. A* **99**, 032316 (2019).
30. A. Tavakoli, D. Rosset, M.-O. Renou, Enabling computation of correlation bounds for finite-dimensional quantum systems via symmetrisation. *Phys. Rev. Lett.* **122**, 070501 (2019).
31. G. M. D'Ariano, P. L. Presti, P. Perinotti, Classical randomness in quantum measurements. *J. Phys. A Math. Gen.* **38**, 5979–5991 (2005).
32. L. Vandenberghe, S. Boyd, Semidefinite programming. *SIAM Rev.* **38**, 49–95 (1996).
33. T. H. Yang, T. Vértesi, J.-D. Bancal, V. Scarani, M. Navascués, Robust and versatile black-box certification of quantum devices. *Phys. Rev. Lett.* **113**, 040401 (2014).
34. J.-D. Bancal, M. Navascués, V. Scarani, T. Vértesi, T. H. Yang, Physical characterization of quantum devices from nonlocal correlations. *Phys. Rev. A* **91**, 022115 (2015).
35. M. Navascués, T. Vértesi, Bounding the set of finite dimensional quantum correlations. *Phys. Rev. Lett.* **115**, 020501 (2015).
36. F. Hirsch, M. T. Quintino, T. Vertesi, M. Navascues, N. Brunner, Better local hidden variable models for two-qubit Werner states and an upper bound on the Grothendieck constant $K_G(3)$. *Quantum* **1**, 3 (2017).
37. L. Guerini, J. Bavaresco, M. Terra Cunha, A. Acin, Operational framework for quantum measurement simulability. *J. Math. Phys.* **58**, 092102 (2017).
38. R. Chaves, J. Bohr Brask, N. Brunner, Device-independent tests of entropy. *Phys. Rev. Lett.* **115**, 110501 (2015).
39. T. Van Himbeeck, E. Woodhead, N. J. Cerf, R. García-Patrón, S. Pironio, Semi-device-independent framework based on natural physical assumptions. *Quantum* **1**, 33 (2017).

40. P. Mironowicz, M. Pawłowski, Experimentally feasible semi-device-independent certification of 4 outcome POVMs. *Phys. Rev. A* **100**, 030301 (2019).

41. R. F. Werner, M. M. Wolf, Bell inequalities and entanglement. *Quantum Inf. Comput.* **1**, 1–25 (2001).

Citation: A. Tavakoli, M. Smania, T. Vértesi, N. Brunner, M. Bourennane, Self-testing nonprojective quantum measurements in prepare-and-measure experiments. *Sci. Adv.* **6**, eaaw6664 (2020).

ARTICLE TOOLS	http://advances.sciencemag.org/content/6/16/eaaw6664
SUPPLEMENTARY MATERIALS	http://advances.sciencemag.org/content/suppl/2020/04/13/6.16.eaaw6664.DC1
REFERENCES	This article cites 41 articles, 0 of which you can access for free http://advances.sciencemag.org/content/6/16/eaaw6664#BIBL
PERMISSIONS	http://www.sciencemag.org/help/reprints-and-permissions